

Responsive Nanoporous Smectic Liquid Crystal Polymer Networks as Efficient and Selective Adsorbents

Huub P. C. van Kuringen, Geert M. Eikelboom, Ivelina K. Shishmanova, Dirk J. Broer,* and Albertus P. H. J. Schenning*

An efficient and selective porous nanostructured polymer adsorbent is prepared from smectic liquid crystals. The adsorption study is performed by using hydrophilic dyes as water pollutants. The anionic pore interior of the nanoporous polymer is able to selectively adsorb cationic methylene blue over anionic methyl orange. Even zwitter ionic rhodamine B could hardly be adsorbed due to the presence of the anionic group in this dye. The confined pore dimensions allow size selective adsorption; a 4th generation cationic dendrimer is not able to diffuse into the nanometer sized pores. The porous nature of the polymer provides easy and fast accessibility of all adsorption sites. Stoichiometric ion exchange is obtained, which equates to an adsorption capacity of nearly 1 gram of methylene blue per 1 gram adsorbent. A competitive Langmuir adsorption constant and pseudo second order rate constant are determined. The adsorbent and adsorbate could both be retrieved after acid treatment of the polymer.

capacities were found for materials based on functionalized biological waste^[13] or clay-polymer composites,^[14] but these materials were not selective. Recently, a charge-selective supramolecular hydrogel^[15] with high adsorption capacity was published, but the adsorption process was slow. Materials which show high selectivity as well as high capacity in combination with a fast adsorption process are practically unavailable.

We have previously reported a fabrication process for nanoporous membranes based on the self-organization of reactive thermotropic hydrogen-bonded smectic liquid crystals (LCs).^[16,17] The membranes were created by photo-polymerization to lock the smectic structure into a network followed by an alkaline treatment to break the hydrogen bonds. Minute interstices are

formed and the smectic nature of the material results in pores with a two-dimensional geometry. Transmission electron microscopy revealed that the width of the straight pores is around 1 nm. A dye was used to measure the local pH in the pores and to prove the porosity. Furthermore, these pores could be filled with silver ions, and subsequently reduced to silver nanoparticles. The diameter and orientation of these nanoparticles were controlled by the pore size and shape of the material.^[18]

This nanoporous material is expected to be a good candidate for an adsorbent material due to the well-organized structure with high surface area and permeability, which promote the adsorption capacity and kinetics. Furthermore, the confined pore interior will be beneficial for selective adsorption. Nanoporous, LC networks have been studied earlier for use as nanoporous membranes,^[19–21] in host-guest chemistry,^[22] molecular imprinting, and chiral recognition. To our knowledge, however, nanoporous materials based on reactive thermotropic liquid crystals have never been considered as selective and fast adsorbents with a high capacity.

1. Introduction

Adsorption is considered to be one of the preferred water treatment methods to purify water due to cost effectiveness.^[1] In addition, adsorption can also be used to recover valuable chemicals in industrial waste streams.^[2] For this purpose, adsorbents with a high selectivity and adsorption capacity are very appealing. Porous and nanostructured materials have gained considerable attention in the past decade as good candidates for adsorption.^[3] The main factors responsible for the outstanding performances of these functional materials are high porosity, low density, high specific surface area, and permeability.^[4]

In the literature, various (porous) materials are described that show selective adsorption, such as silica,^[5] hydrogels,^[6–10] or metal-organic frameworks (MOFs).^[11,12] High adsorption

H. P. C. van Kuringen, G. M. Eikelboom,
Dr. I. K. Shishmanova, Prof. D. J. Broer,
Prof. A. P. H. J. Schenning
Functional Organic Materials and Devices
and Institute for Complex Molecular Systems
Department of Chemical Engineering and Chemistry
Eindhoven University of Technology
Den Dolech 2, 5600 MB, Eindhoven, The Netherlands
E-mail: D.Broer@tue.nl; A.P.H.J.Schenning@tue.nl

H. P. C. van Kuringen
Dutch Polymer Institute (DPI)
PO Box 902, 5600 AX, Eindhoven, The Netherlands

DOI: 10.1002/adfm.201400428



2. Results and Discussion

2.1. Preparation and Characterization of a Smectic Liquid Crystalline Network

The LC mixture with 4-(6-acryloyloxyhexyloxy)benzoic acid (6OBA) and 1,4-phenylene bis(4-(6-(acryloyloxy)hexyloxy)

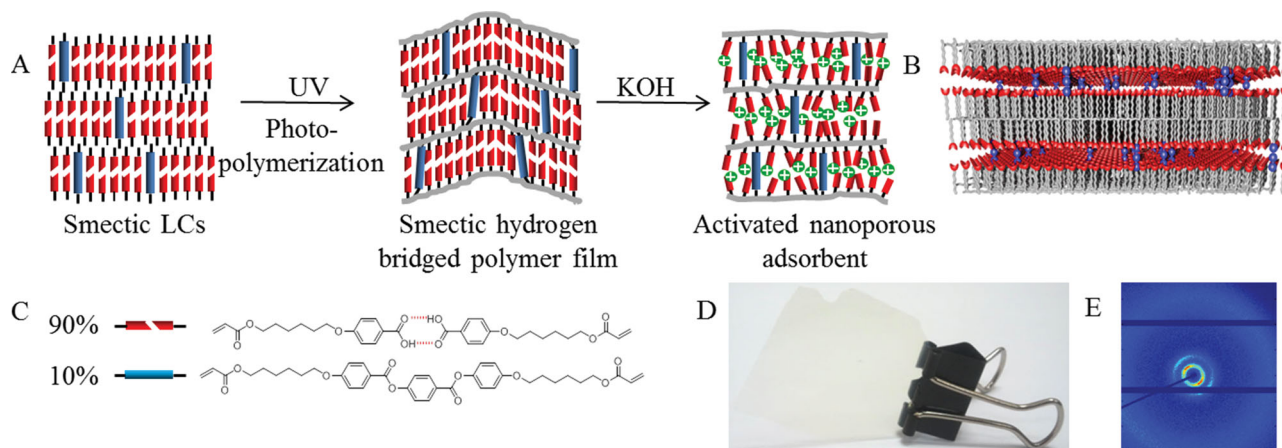


Figure 1. (A) Schematic representation of the formation of the nanoporous adsorbent based on smectic liquid crystals. (B) Simplified artistic view of the nanopores in the layered network. To visualize the 2D pores the counter ion is not shown and the benzoic acid derivatives are drawn highly ordered. (C) The chemical structure of the LCs. (D) Free standing hydrogen bridged polymer film. (E) X-ray diffraction of smectic activated adsorbent.

benzoate (C₆H) (Figure 1) in a 9/1 w/w ratio was characterized. The mixture melts at 90 °C to become smectic A. A careful look revealed a cybotactic nematic phase above 101 °C that was not assigned previously^[16–18] and at 110 °C it becomes isotropic. The mixture was photo-polymerized in the smectic phase at 95 °C which resulted in a planar aligned free standing smectic film of approximately 2.5 cm × 2.5 cm × 18 μm in size. Fourier-transform infrared spectroscopy (FTIR) was used to confirm the conversion of the acrylate groups.

The hydrogen bridged network and base treated network were characterized with thermogravimetric analysis (TGA), X-ray photoelectron spectroscopy (XPS), and FTIR to determine the composition of the material. The TGA graph showed an absence of inorganic compounds in the case of the hydrogen bridged film. The KOH treated polymer salt film revealed an inorganic fraction of 17.4% which is close to the predicted value of 19.0% assuming that all carboxylic acid was converted to carboxylate anions with potassium counter ions. XPS also showed the compound composition, which is close to the theoretical predicted values for both films. The formation of the polymer salt was investigated with FTIR, which revealed the absence of hydrogen bridges. Polarized optical microscopy (POM) and X-ray diffraction (XRD) pictures (Figure 1E) confirmed that the smectic anisotropic network is maintained after the base treatment. A d-spacing of 3.3 nm was observed (Supporting Information, Figure S7), which is in agreement with earlier observations.^[16]

2.2. Methylene Blue Adsorption

To investigate the adsorption behavior of the liquid crystalline polymer network, 5 mL methylene blue (MB) solution (5.0 μg mL⁻¹, 15.6 μM) was prepared and both a colorless transparent film freshly treated with base (0.74 mg) as well as an untreated film

(0.85 mg) were allowed to adsorb the cationic dye. Some color changes were observed by the naked eye. The solution containing the base treated film became gradually less blue and the film appeared blue. After 5 h, the solution was completely colorless while the film was darkly colored (blue), indicating that the polymer film had adsorbed the cationic dye from the solution. In contrast, the hydrogen bridged polymer film that had not been treated with the alkaline solution did not become colored. Absorbance spectra were recorded of the solution with UV-vis spectroscopy to quantify the adsorption, which confirmed the absence of dye in the solution with the activated adsorbent (Figure 2). The solution with the hydrogen bridged film had nearly the same absorbance as the initial dye solution, revealing its inability to adsorb the cationic dye. This suggests that the adsorption is based on an ionic interaction. The cationic dye is able to be adsorbed in the anionic interior of the material. If this anionic interior is absent, as in the case of the hydrogen bridged state, the cationic dye cannot be adsorbed. Furthermore, the polymer salt film is able to adsorb all MB from the solution and calculations reveal a MB/carboxylate ratio of 0.04 mole/mole. This indicates that the material is not yet saturated and could possibly adsorb higher amounts of MB.

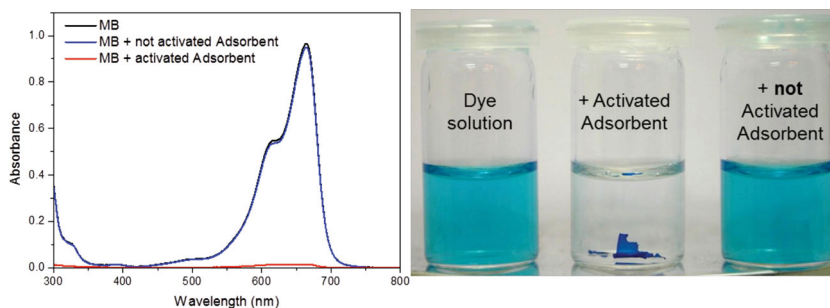


Figure 2. Adsorption of MB in the nanoporous adsorbent. Left: UV-vis spectra of the dye solutions before and after it was added to the activated or non-activated adsorbent. Right: vials with the initial dye solution on left hand side, the dye solution with the activated adsorbent in the middle and the non-activated adsorbent on the right.

2.3. Adsorption Capacity

To investigate the maximum adsorption capacity for this material, the adsorbent was exposed to a solution with a higher concentration of MB. Since the adsorption is based on ionic interactions different MB/carboxylate ratio were chosen between 0.04 and 2. The total volume of the dye solution was kept constant at 5 mL. To be sure that adsorption equilibrium is reached the dye concentration in solution was recorded for 3 days.

The solutions and films were visually inspected. The solutions up to a MB/carboxylate ratio of 0.88 all became almost colorless, indicating adsorption of the MB. The solutions with a higher ratio became less blue but not colorless. The films became darker blue when they had adsorbed more MB and at a certain point they even appear black,^[23] caused by combination of the high dye concentration in the film and the absorbance of MB in the visual area.^[23,24] The dye concentrations in these solutions were determined by UV-vis spectroscopy and the amount of adsorbed dye was calculated using Equation (1) (see the Experimental Section; see also Figure 3). A straight line is observed up to a ratio of almost 1, indicating full adsorption, which was expected since these solutions became colorless at equilibrium. Saturation is obtained at an occupation degree of 100% when all carboxylate moieties are occupied with a MB molecule. Surprisingly, only a small excess of dye is necessary to reach complete occupation, meaning that the affinity between methylene blue and the adsorbent is high.

At 100% occupation, the adsorption capacity is 980 mg of MB for 1 g of material. The nanoporous LC network can adsorb 30 times more than the well-known adsorbent, activated carbon.^[25] However, a poly(acrylic acid) based hydrogel^[14] was able to adsorb even more MB. This is caused by the lower molecular mass of acrylic acid with respect to the benzoic acid derivative in our network.

The adsorption equilibrium data can be fitted well to the Langmuir adsorption isotherm.^[26] This isotherm is based on the assumption that the adsorbent has a specific number of independent active sites that can bind a finite number of molecules. The best fit was obtained with an adsorption capacity of 1.00 mole/mole. This means that all sites are reachable for MB and to achieve this, the material has to be sufficiently porous and there cannot be steric limitations. In comparison, the adsorption capacity for the poly(acrylic acid) based hydrogel^[14]

is only 0.45 mole/mole. The obtained Langmuir adsorption constant is $3.42 \times 10^{-4} \text{ L mg}^{-1}$ ($0.363 \text{ L } \mu\text{mol}^{-1}$) for our LC network which is much higher than for the poly(acrylic acid) based hydrogel ($6.36 \times 10^{-5} \text{ L mg}^{-1}$).^[14] This means that the binding affinity is more than 5 times higher for this LC adsorbent.

The MB filled adsorbent was characterized with TGA, XPS, and FTIR to determine the composition of the material. The TGA (Supporting Information, Figure S8) showed an absence of potassium or other inorganic salts. XPS (Supporting Information, Figure S9) showed a compound composition close to the expected value; no potassium was observed and, interestingly, the spectrum revealed the absence of chloride, which could be present as counter ion from MB. These results confirm the earlier statement that the adsorption is based on an ionic interaction and the material can adsorb MB until all potassium is exchanged. The absence of chloride in the material showed that the adsorbent is possibly charge selective. FTIR spectroscopy (Supporting Information, Figure S10) revealed the absence of hydrogen bridges between carboxylic acid moieties in the adsorbent. This is expected, because all carboxylate moieties are occupied with MB.^[27]

Additionally, a tetra cationic dye was adsorbed to confirm the proposed ion exchange mechanism. A porphyrin derivative with 4 cationic moieties was dissolved in 5 mL water (0.73 mg mL^{-1} , 0.8 mM) and the activated adsorbent was added with a 2/1 ratio of dye over carboxylate moieties. A decrease of this dye in solution was observed and UV-vis spectroscopy revealed that 10.5% of the dye is adsorbed. Meaning that 84% of the carboxylate moieties is occupied with a cationic group of the multivalent dye.

2.4. Adsorption Kinetics

The adsorption kinetics were investigated by measuring the absorbance of the solution over time (Figure 3). The absorbance of the reference MB solution did not significantly change, and therefore (photo-)reduction of MB can be neglected.^[28,29] The data were fitted to both pseudo-first order and pseudo-second order kinetics. It reveals that the pseudo-second order equation fits the adsorption kinetics well: the correlation coefficient is very high ($R^2 = 0.9987$). The pseudo-second order kinetic is often found when studying the adsorption of MB,^[8,14,15,30] and supports the view that ionic interactions between the LC

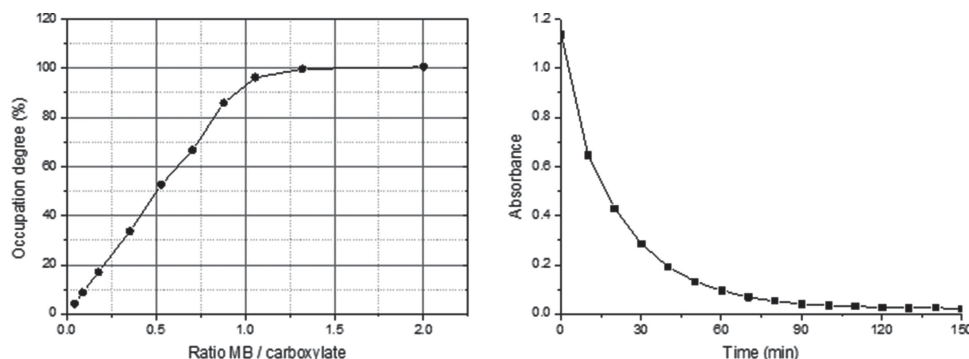


Figure 3. MB adsorption in the nanoporous adsorbent. Left: Occupation degree of carboxylate moieties in the adsorbent at different MB/carboxylate ratios. Right: MB adsorption over time.

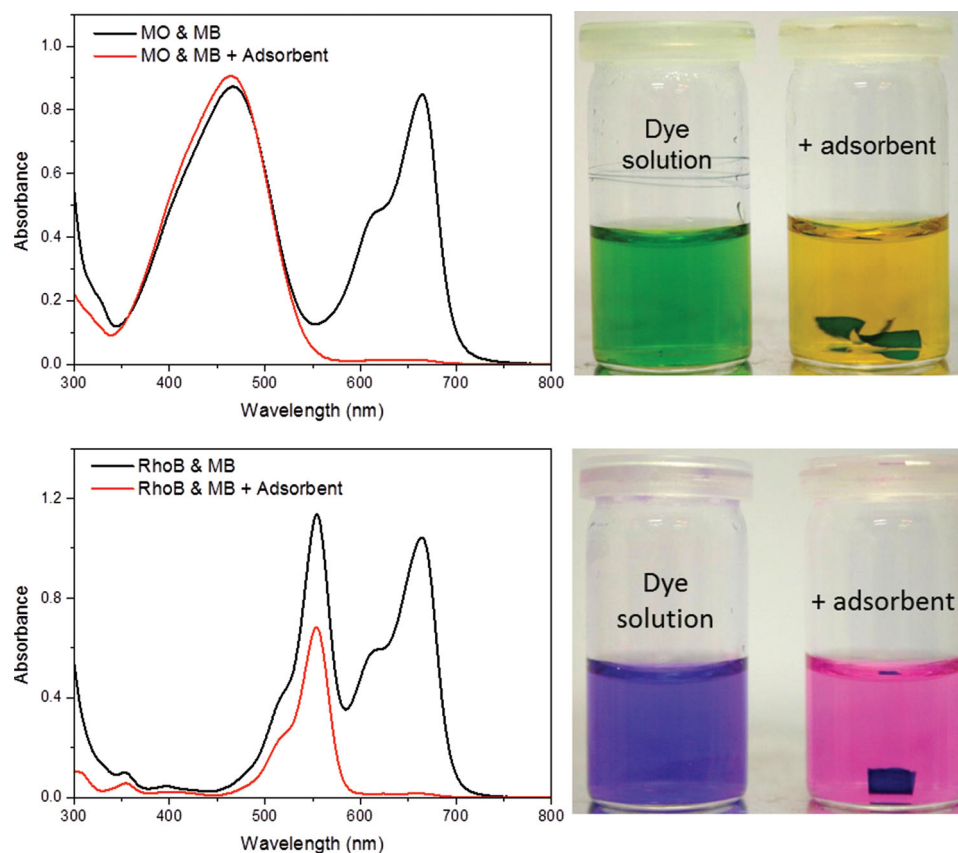


Figure 4. Charge selective adsorption of cationic MB over anionic MO and zwitterionic RhoB. Top: MO and MB. Bottom: RhoB and MB. Left: UV-vis spectra before and after adsorption. Right: Vials of the initial dye solution and after adsorption.

network and MB are occurring.^[15] The rate constant of our adsorbent is 2.89×10^{-3} g adsorbent (mg MB min)⁻¹. Such a high rate constant has not been reported before for materials which also have a high adsorption capacity. The rate constant is 5 times faster than poly(acrylic acid) based hydrogel^[14] at 0.575×10^{-3} g/(mg min) and nearly 2000 times faster than a supramolecular hydrogel^[15] (1.5×10^{-6} g/(mg min)).

2.5. Selective Adsorption of Hydrophilic Dyes

To investigate selective adsorption a competitive experiment was performed. A solution was made with an anionic and cationic dye, which have quite similar molecular dimensions. $12.9 \mu\text{g mL}^{-1}$ ($39.4 \mu\text{M}$) anionic methyl orange (MO) and $5.0 \mu\text{g mL}^{-1}$ ($15.6 \mu\text{M}$) cationic blue MB were dissolved in distilled water, which resulted in a green solution. The UV-vis spectrum of the solution revealed two peaks, one with a peak maximum at 465 nm belonging to MO and the second absorbance peak at 665 nm belonging to MB. Excess of nanoporous adsorbent was added to this mixture and was allowed to adsorb the dyes. After 5 h, a yellow solution was observed and a blue adsorbent. The UV-vis spectra of the solution was recorded which reveals the same absorbance peak of MO as the initial solution, while the MB peak is hardly visible (Figure 4). This evidences that charge selective adsorption is possible with this adsorbent.

Subsequently, a solution was made with zwitterionic rhodamine B (RhoB) and MB. RhoB has a permanent positive charge and under the conditions used the acid group is deprotonated, which results in a negative charge as well. This zwitterion was dissolved in distilled water ($5.0 \mu\text{g mL}^{-1}$, $10.4 \mu\text{M}$) together with $5.0 \mu\text{g mL}^{-1}$ MB ($15.6 \mu\text{M}$) and excess of adsorbent was added. This resulted in a purple solution which gradually became pink and the adsorbent became blue/purple (Figure 4). The UV-vis spectrum reveals the disappearance of MB signal, while the RhoB absorbance peak at 554 nm is only reduced. This reduction is caused by the disappearance of the overlapping MB absorbance peak and the slight adsorption of RhoB in the adsorbent. A single MB absorbance peak was subtracted from this spectrum and revealed an RhoB adsorption of 33%, while MB is adsorbed for at least 99%. The small pores in the adsorbent only allow dyes with cationic groups to get adsorbed and have strong preference for ions with solely cationic groups. The restricted pore size in the adsorbent might be used to have selective adsorption of small cations over bigger cations. A commercially available 4th generation poly(propylene imine) dendrimer^[31] (FITC-Dend), which was modified with glycol galate end groups, quarternized interior, with 30 cationic moieties and fluorescein isothiocyanate (FITC) label to become detectable for UV-vis spectroscopy was selected. The adsorbent was added to a mixture of $5.0 \mu\text{g mL}^{-1}$ MB ($15.6 \mu\text{M}$) and $168 \mu\text{g mL}^{-1}$ ($0.029 \mu\text{M}$) FITC-Dend. An excess of adsorbent was added

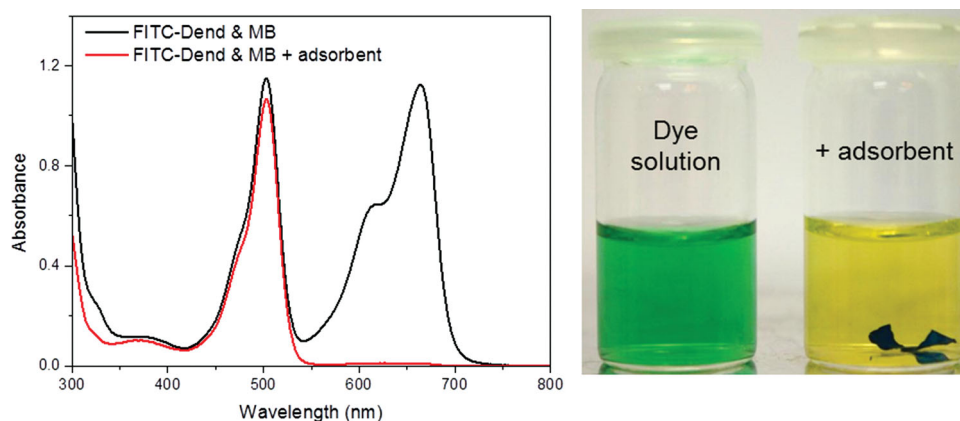


Figure 5. Size selective adsorption of small MB over large FITC-Dend. Left: UV-vis spectrum before and after adsorption. Right: Vials of the initial dye solution and after adsorption.

to the green solution, which slowly became yellow, while the adsorbent became blue (**Figure 5**), indicating that size-selective adsorption took place. The UV-vis spectrum confirms the size selective adsorption of the small MB over the larger dendrimer. A similar experiment was carried out with a 2nd generation dendrimer, the adsorbent became yellow and UV-vis spectroscopy revealed a decrease of this dye in solution, indicating the adsorption of this smaller sized dendrimer. It should be noted that due to the flexible nature of the dendrimer the dimensions are unknown, but they are at least bigger as the MB, which is approximately 1 nm in size.

2.6. Desorption

Desorption is important to re-use the adsorbent or to win back valuable adsorbates. This was investigated with fresh, completely MB filled adsorbent in distilled water. The solution became only slightly blue, indicating a minor desorption of MB. The adsorbent is able to hold the major fraction of the MB at neutral pH. However, after the addition of 0.1 mL 4 M HCl the solution suddenly became blue indicating desorption of MB (**Figure 6**). IR spectroscopy revealed the presence of the hydrogen bridges in the adsorbate while the signals of the carboxylate salt peak were

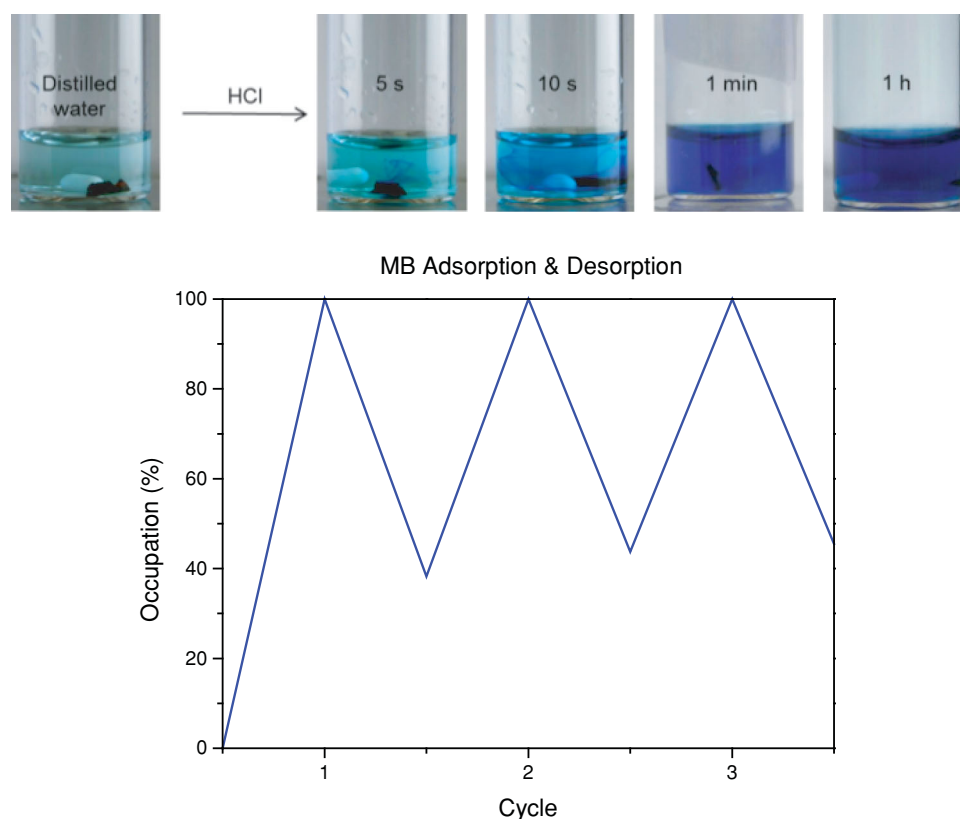


Figure 6. Top: Desorption of MB hardly occurs in distilled water (left). After the addition of acid, desorption occurs (right). Bottom: Occupation degree of adsorption sites with MB during three cycles of adsorption and desorption.

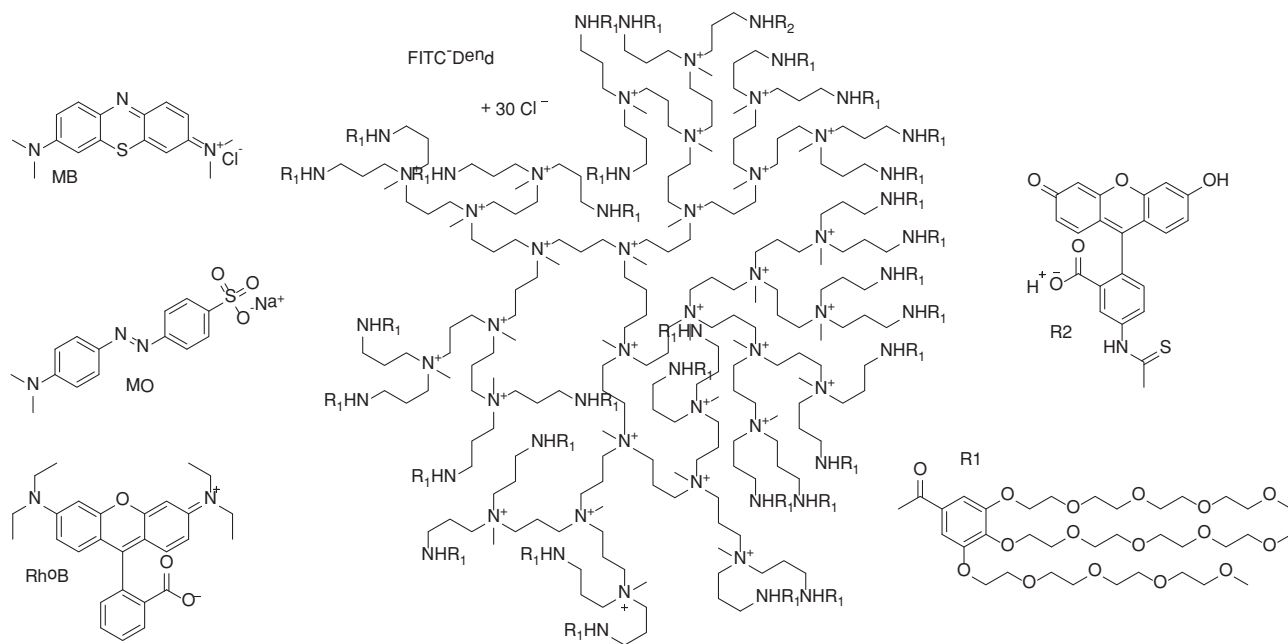


Figure 7. Dyes used in the adsorption study; cationic methylene blue (MB), anionic methyl orange (MO), zwitterionic rhodamine B (RhoB) and 4th generation poly(propylene imine) dendrimer (FITC-Dend),^[31] which was modified with glycol gallate end groups, quarternized interior and fluorescein isothiocyanate (FITC) label.

hardly observed. At low pH the carboxylate moieties are protonated and MB is removed from the adsorbent. Additionally, the adsorption and desorption was investigated multiple times. The activated adsorbent was placed in neutral water containing MB and subsequently immersed in pH 1 HCl solution to adsorb and desorb MB, respectively. The adsorption and release was quantified with UV-vis spectroscopy, which revealed that up to 60% of the MB was released in every cycle. The adsorption and desorption is reversible in three repeating cycles (Figure 6), indicating that the adsorbent can be used many times.

3. Conclusion

A nanoporous network is prepared based on reactive smectic liquid crystals. After base treatment the adsorbent is activated and is able to very efficiently adsorb cationic dyes and to selectively adsorb cationic dyes over anionic, zwitter ionic and larger cations. The adsorption is based on the ion-exchange and all counter ions can be exchanged, which resulted in a very high adsorption capacity of nearly 1 gram MB for 1 gram adsorbent. The adsorption follows the Langmuir isotherm and pseudo-second order kinetic model and the study reveals high values for the Langmuir adsorption and rate constants, which are very competitive with other promising adsorbents. The adsorbate can be released by acid treatment, which makes the re-use of adsorbate or the recovery of valuable adsorbates possible.

Currently, we are investigating nanoporous smectic liquid crystalline networks with adjustable pore dimensions and chemical interior for controlled selective adsorption. Furthermore, we are investigating the possibility to make polymer

liquid crystal beads to easily apply these materials for separation, adsorption and purification purposes.

4. Experimental Section

Materials: The hydrogen bridged 4-(6-acryloyloxyhexyloxy)benzoic acid and the liquid crystalline crosslinker, 1,4-phenylene bis(4-(6-(acryloyloxy)hexyloxy) benzoate) were both custom made by Synthon Chemicals, Germany. Initiator 1-hydroxycyclohexylphenylketone (Irgacure 184) was supplied by Ciba Specialty Chemicals, inhibitor p-methoxyphenol was purchased from Aldrich.

Preparation of the Liquid Crystalline Network: A LC mixture was made with the hydrogen bridged 6OBA, and the covalently bonded crosslinker; C6H in a 90/10 w/w ratio. In order to make the mixture accessible for photopolymerization 0.5 wt% 1-hydroxycyclohexylphenylketone was added as photoinitiator. For stabilization, 0.1 wt% of p-methoxyphenol was added as thermal polymerization inhibitor. A mixture was made by dissolving the compounds together in dichloromethane, which was subsequently evaporated, and characterized with Differential Scanning Calorimetry (DSC), POM and XRD.

Films with a thickness that varied between 15 and 20 μm were made by processing the mixture in the melt at 105 $^{\circ}\text{C}$ by capillary suction between two accurately spaced glass plates. To get planar alignment the glass plates were provided with rubbed polyimide (OPTMER AL 1051, JSR Corporation, Tokyo, Japan). The photo-polymerization in the smectic state of the monomers was performed at 95 $^{\circ}\text{C}$ for 5 min with a mercury lamp (Omnicure s1000) at the intensity of approximately 5 mW cm^{-2} at the sample surface followed by a heat treatment at 135 $^{\circ}\text{C}$ to ensure maximum conversion of the acrylate groups.

Dye Adsorption: For adsorption experiments hydrophilic dyes were chosen (Figure 7). The dyes were dried prior to use and dissolved at a known concentration in distilled water to get a relative absorbance of approximately 1. The hydrogen bridged polymer film was cut into small pieces of approximately 0.6–1.0 mg. The polymer films were immersed in

5 mL 0.05 M KOH solution to deprotonate the carboxylic acid moieties, which results in rupture of the hydrogen bridges and formation of the polymer salt. They were quickly washed with a few milliliters of distilled water to remove the residual base and, subsequently, the dye solution was added to the polymer film. The films were allowed to adsorb dye at 20 °C until reaching equilibrium. The solutions were mixed by a magnetic stirring bar or by using a shaking plate.

Adsorption is usually calculated by dividing the weight of adsorbate by the weight of adsorbent.^[8–10,13,14] In our liquid crystal network the adsorption capacity can be clearly determined by the amount of carboxylate moieties, which is related to the initial concentration of the hydrogen bonded dimer molecules in the LC mixture. The adsorption will be expressed as the number of moles of adsorbate by the number of carboxylate moieties. The expression to calculate this is shown in (Equation (1)).

$$q = \frac{(c_i - c_f)V}{n_m} \times 100\% \quad (1)$$

where q (mol/mol) is the amount of dye per amount of carboxylate moieties in the polymer film, c_i and c_f (mol L⁻¹) are the concentrations of dye in solution before and after adsorption, respectively, V (L) is the volume of the dye solution and n_m (mol) is the amount of carboxylate moieties. The adsorption behavior was monitored by UV-vis spectroscopy, and the dye concentration was calculated using the peak maximum. A calibration curve was made to be sure that extinction coefficient remains constant over a large concentration range, i.e., does not change over 0.1 up to 1.5 absorbance which might change due to aggregation of methylene blue.^[32]

Supporting Information

Supporting Information is available from the Wiley Online Library or from the author.

Acknowledgements

This research forms part of the research programme of the Dutch Polymer Institute (DPI), project 742. We would like to thank Henk Janssen from SyMo-Chem B. V. for kindly supplying the dendrimer, Tiny Verhoeven for performing the XPS measurements and Giuseppe Portale for the help with the X-ray measurements.

Received: February 7, 2014

Revised: March 21, 2014

Published online: May 13, 2014

[1] I. Ali, *Chem. Rev.* **2012**, *112*, 5073.

[2] M. A. Shannon, P. W. Bohn, M. Elimelech, J. G. Georgiadis, B. J. Marinas, A. M. Mayes, *Nature* **2008**, *452*, 301.

- [3] I. Mohmood, C. B. Lopes, I. Lopes, I. Ahmad, A. C. Duarte, E. Pereira, *Environ. Sci. Pollution Res.* **2013**, *20*, 1239.
- [4] Y. Ning, Y. Yang, C. Wang, T. Ngai, Z. Tong, *Chem. Commun.* **2013**, *49*, 8761.
- [5] K. Y. Ho, G. McKay, K. L. Yeung, *Langmuir* **2003**, *19*, 3019.
- [6] R. Wang, B. Yu, X. Jiang, J. Yin, *Adv. Funct. Mater.* **2012**, *22*, 2606.
- [7] B. Li, X. Jiang, J. Yin, *J. Mater. Chem.* **2012**, *22*, 17976.
- [8] S. Deng, H. Xu, X. Jiang, J. Yin, *Macromolecules* **2013**, *46*, 2399.
- [9] S. Deng, R. Wang, H. Xu, X. Jiang, J. Yin, *J. Mater. Chem.* **2012**, *22*, 10055.
- [10] A. T. Paulino, M. R. Guilherme, A. V. Reis, G. M. Campese, E. C. Muniz, J. Nozaki, *J. Colloid Interface Sci.* **2006**, *301*, 55.
- [11] C.-Y. Sun, X.-L. Wang, C. Qin, J.-L. Jin, Z.-M. Su, P. Huang, K.-Z. Shao, *Chem.-Eur. J.* **2013**, *19*, 3639.
- [12] F. Pu, X. Liu, B. L. Xu, J. S. Ren, X. G. Qu, *Chem.-Eur. J.* **2012**, *18*, 4322.
- [13] M. A. M. Salleh, D. K. Mahmoud, W. A. W. A. Karim, A. Idris, *Desalination* **2011**, *280*, 1.
- [14] Y. Liu, Y. A. Zheng, A. Q. Wang, *J. Environ. Sci. China* **2010**, *22*, 486.
- [15] B. O. Okesola, D. K. Smith, *Chem. Commun.* **2013**, *49*, 11164.
- [16] C. L. Gonzalez, C. W. M. Bastiaansen, J. Lub, J. Loos, K. Lu, H. J. Wondergem, D. J. Broer, *Adv. Mater.* **2008**, *20*, 1246.
- [17] I. K. Shishmanova, C. W. M. Bastiaansen, A. P. H. J. Schenning, D. J. Broer, *Chem. Commun.* **2012**, *48*, 4555.
- [18] D. Dasgupta, I. K. Shishmanova, A. Ruiz-Carretero, K. Lu, M. W. G. M. Verhoeven, H. P. C. van Kuringen, G. Portale, P. Leclerc, C. W. M. Bastiaansen, D. J. Broer, A. P. H. J. Schenning, *J. Am. Chem. Soc.* **2013**, *135*, 10922.
- [19] D. L. Gin, X. Lu, P. R. Nemade, C. S. Pecinovsky, Y. Xu, M. Zhou, *Adv. Funct. Mater.* **2006**, *16*, 865.
- [20] A. P. H. J. Schenning, Y. C. Gonzalez-Lemus, I. K. Shishmanova, D. J. Broer, *Liquid Crystals* **2011**, *38*, 1627.
- [21] H. Zhang, L. Li, M. Moller, X. M. Zhu, J. J. H. Rueda, M. Rosenthal, D. A. Ivanov, *Adv. Mater.* **2013**, *25*, 3543.
- [22] Y. Ishida, *Materials* **2011**, *4*, 183.
- [23] Remarkably, an orange/red reflection appears if high amounts of MB are adsorbed.
- [24] A. J. Chung, M. F. Rubner, *Langmuir* **2002**, *18*, 1176.
- [25] C. Sarici-Ozdemir, *Physicochem. Problems Mineral Process.* **2012**, *48*, 441.
- [26] Y. Liu, *Colloids Surf. A-Physicochem. Engin. Aspects* **2006**, *274*, 34.
- [27] The pH of the initial MB solutions (pH 7) were below the pKa of the adsorbent (pKa 8.5), indicating that the solution does not need to be adjusted to pH 8.5 or higher.
- [28] Y. Usui, M. Koizumi, *Bull. Chem. Soc. Japan* **1961**, *34*, 1651.
- [29] G. Somer, M. E. Green, *Photochem. Photobiol.* **1973**, *17*, 179.
- [30] T. S. Anirudhan, A. R. Tharun, *Chem. Engin. J.* **2012**, *181*, 761.
- [31] F. Tack, A. Bakker, S. Maes, N. Dekeyser, M. Bruining, C. Elissen-Roman, M. Janicot, M. Brewster, H. M. Janssen, B. F. M. De Waal, P. M. Fransen, X. Lou, E. W. Meijer, *J. Drug Targeting* **2006**, *14*, 69.
- [32] B. Liu, L. Wen, K. Nakata, X. Zhao, S. Liu, T. Ochiai, T. Murakami, A. Fujishima, *Chem.-Eur. J.* **2012**, *18*, 12705.